

Article

# Estimating Time of Concentration for Overland Flow on Pervious Surfaces by Particle Tracking Method

Xiaoning Li <sup>1</sup>, Xing Fang <sup>1,2,\*</sup> , Junqi Li <sup>2</sup>, Manoj KC <sup>3</sup> , Yongwei Gong <sup>2</sup> and Gang Chen <sup>4</sup><sup>1</sup> Department of Civil Engineering, Auburn University, Auburn, AL 36849-5337, USA; xz10055@auburn.edu<sup>2</sup> Key Laboratory of Urban Stormwater System and Water Environment, Ministry of Education, Beijing University of Civil Engineering and Architecture, Beijing 100044, China; lijunqi@bucea.edu.cn (J.L.); gongyongwei@bucea.edu.cn (Y.G.)<sup>3</sup> Billingsley Engineering, Las Vegas, NM 87701, USA; manoj@billingsleyengineering.com<sup>4</sup> College of Hydrology and Water Resources, Hohai University, No. 1 Xikang Road, Nanjing, Jiangsu 210098, China; gangchen@hhu.edu.cn

\* Correspondence: xing.fang@auburn.edu; Tel.: +1-334-844-8778; Fax: +1-334-844-6290

Received: 5 February 2018; Accepted: 23 March 2018; Published: 25 March 2018



**Abstract:** The particle tracking method (PTM) module was added into the open source Full Shallow-Water equations for Overland Flow in a two-dimensional (FullSWOF\_2D) program, which has coupled rainfall–runoff and infiltration modules to determine the time of concentration ( $T_c$ ) for impervious ( $T_{ci}$ ) and pervious ( $T_{cp}$ ) surfaces. The updated program FullSWOF-PTM was tested using observed rainfall events with Nash–Sutcliffe efficiencies ranging from 0.60 to 0.95 (average of 0.75) for simulated runoff hydrographs. More than 400 impervious modeling cases with different surface slope ( $S_0$ ), roughness coefficient ( $n$ ), length ( $L$ ), and rainfall intensity ( $i$ ) combinations were developed and simulated to obtain the  $T_{ci}$  for developing the regression equation of  $T_{ci}$  as a function of the four input parameters. More than 700 pervious modeling cases with different combinations of  $S_0$ ,  $n$ ,  $L$ ,  $i$ , and infiltration parameters including the saturated hydraulic conductivity, suction head, and moisture deficit were simulated to estimate the  $T_{cp}$  based on the travel time of 85% of particles arriving at the outlet and the ponding time. The regression equation of  $T_{cp}$  was developed as the sum of  $T_{ci}$  and additional travel time as a function of infiltration parameters and  $i$ . The  $T_{cp}$  equation can be applied to wide ranges of input parameters in comparison to Akan's equation.

**Keywords:** pervious surfaces; time of concentration; overland flow model; particle tracking method

## 1. Introduction

Mulvaney [1] first put forward the concept of time of concentration ( $T_c$ ) and Kuichling [2] defined  $T_c$  as the time needed for the runoff from the most remote part of a catchment to travel to the outlet during the rainfall–runoff process. It is widely used to design the highway and urban stormwater drainage facilities [3] using  $T_c$  as design rainfall duration [4]. There are dozens of studies where researchers developed and tested/compared  $T_c$  equations [5,6]. They obtained the  $T_c$  estimation using hydrograph analysis for laboratory plots/watersheds [7–9], theoretical derivation based on kinematic wave theory [4,10–12], and distributed physically-based numerical simulation programs utilizing topographic elevation and geometric data [13–16]. Izzard [7] developed a method to calculate the runoff hydrography and the time necessary to substantially reach an equilibrium of flow resulting from given rainfall intensity, roughness, slope, and the length of the overland flow plan based on the laboratory experiments. Compared to laboratory analysis and theory deduction, the distributed and physically-based numerical models solving the shallow-water equations (SWEs) are more and more widely used in overland flow simulation for its better performance dealing with

mixed subcritical and supercritical flow compared to kinematic wave and diffusive wave approach or other approximation [17,18]. Su and Fang [15] established a two-dimensional numerical model based on shallow-water equations to estimate traveling time for different rainfall intensity, roughness, length, and slope modeling cases and developed the travel time estimation equation for relatively steep and very flat watersheds. Recently, more and more researchers moved their focus to the overland flow of pervious surfaces [19–22]. Hjelmfelt [23] analyzed the infiltration influence on the overland flow by combining the storage–depletion model of the U.S. Soil Conservation Service with the kinematic wave equations and found the variation of infiltration rate during a storm had a significant effect on the time of concentration and on the shape of the runoff hydrograph. In Guo’s study [4], the Wooding’s solution was expanded to overland flow on pervious surfaces by coupling the kinematic wave equations with the Horton infiltration model. Only Akan developed a time of concentration calculation chart [10] and a formula [24] using Manning’s friction law on rectangular pervious plots under constant-intensity rainfall based on the kinematic wave equations and Green–Ampt (GA) infiltration model. The time of concentration in Akan’s study was measured from the beginning of the rainfall event, which meant the ponding time ( $t_p$ ) and runoff travel time were lumped together in the formula. The chart and formula are mainly appropriate for the cases when Manning’s friction law is acceptable and there are limited ranges of rainfall and soil infiltration parameters. Further work is still needed, e.g., to expand the formula to other flow resistance laws and wide ranges of rainfall and soil infiltration parameters.

Conceptually, the time of concentration is when the entire catchment becomes contributory to the runoff at the outlet, but there are various methods that have been developed/used to estimate  $T_c$ .  $T_c$  for impervious areas ( $T_{ci}$ ) was typically estimated from hydrograph analysis, e.g.,  $T_{ci}$  as lapsed time from the beginning of a rainfall event to the outlet flow reaching 98% of the peak discharge, which is called  $T_{c-q98}$  hereafter, since the runoff starts immediately after the rainfall, and  $T_c$  and the runoff equilibrium time are basically the same for impervious surfaces. The above method does not work for determining the time of concentration on pervious surfaces ( $T_{cp}$ ) since the runoff does not start before the ponding time ( $t_p$ ) and then discharge increases asymptotically to peak or equilibrium discharge under constant rainfall intensity even after a long period of simulation. Guo [4] suggested evaluating  $T_{cp}$  of a small catchment by velocity-based methods rather than those empirical formulas developed for and calibrated by the observed hydrographs. The particle tracking method (PTM) is popular for generating path lines and travel time information since it directly utilizes the simulated velocity field results [25–28]. KC and Fang [29] developed a quasi-two-dimensional (2D) diffusion wave model (DWM) coupled with particle tracking to determine the time parameters including the travel time for 85%, 95%, and 100% of particles to arrive at the outlet ( $T_{r-p85}$ ,  $T_{r-p95}$ ,  $T_{r-p100}$ ) of overland flow on impervious surfaces. These travel times have significant linear correlations with each other and a significant agreement between the  $T_{r-p85}$  and  $T_{c-q98}$  was found.

To understand and estimate  $T_{cp}$  for pervious surfaces is particularly important and useful to smart stormwater management using the lower impact development (LID) and green infrastructures (GI) that promote the infiltration [22]. Therefore, the goal of this study is to develop a  $T_{cp}$  equation for pervious surfaces that can be applied to wide ranges of rainfall, watershed, and soil parameters. First, the PTM module was added into the open source Full Shallow-Water equations for Overland Flow in a two-dimensional (FullSWOF\_2D, version 1.07, Lab. J. A. Dieudonné & EPU Nice Sophia, Nice, France) [30] program for determining  $T_{cp}$  for pervious surfaces. The FullSWOF\_2D program has already coupled the rainfall–runoff modules with the infiltration module [29] for possibly exploring  $T_{cp}$  after adding the PTM module (called FullSWOF-PTM). A total of 750 pervious modeling cases that are combinations of diverse values of rainfall intensity  $i$  (m/s or mm/h), watershed slope  $S_0$ , Manning’s roughness coefficient  $n$ , length  $L$  (m), hydraulic conductivity  $K$  (m/s), suction head  $\phi$  (m), and moisture deficit  $\Delta\theta$  of pervious surfaces were generated considering different types of soil groups. Travel time for 85% of particles arriving at the outlet from the beginning of rainfall, which is determined using FullSWOF-PTM and called  $T_{r-p85}$  hereafter, was used directly to evaluate  $T_{ci}$  for impervious surfaces, and the  $T_{r-p85}$  subtracting the ponding time  $t_p$  was used to evaluate  $T_{cp}$  for pervious surfaces, which is

consistent with Guo's study [4] but different from Akan's equation [24]. The multiple linear regression (MLR) method was used to derive the  $T_{ci}$  and  $T_{cp}$  equations as a function of input parameters.

## 2. Materials and Methods

### 2.1. Shallow Water Equations (SWEs) and FullSWOF\_2D

As a Saint-Venant system [31], the simplified SWEs model is widely used to simulate the incompressible Navier–Stokes flow occurring in rivers, channels, ocean, and land surfaces [32]. It is derived with two assumptions: one is that the fluid velocity is constant along the vertical ( $z$ ) direction and that the water depth is small with respect to the horizontal ( $x, y$ ) dimensions; another is that the pressure of the fluid is hydrostatic ( $\partial p/\partial z = -g$ ), which means the pressure field could be calculated with simple integration along the vertical ( $z$ ) direction [30,33]. The conservative form of the 2D SWEs including the continuity equation and two momentum equations for  $x$  and  $y$  directions are stated as the following equations:

$$\frac{\partial h}{\partial t} + \frac{\partial hu}{\partial x} + \frac{\partial hv}{\partial y} = R - I \quad (1)$$

$$\frac{\partial hu}{\partial t} + \frac{\partial}{\partial x} \left( hu^2 + \frac{gh^2}{2} \right) + \frac{\partial}{\partial y} (huv) = -gh \left( \frac{\partial z}{\partial x} + S_{fx} \right) \quad (2)$$

$$\frac{\partial hv}{\partial t} + \frac{\partial}{\partial x} (huv) + \frac{\partial}{\partial y} \left( hv^2 + \frac{gh^2}{2} \right) = -gh \left( \frac{\partial z}{\partial y} + S_{fy} \right) \quad (3)$$

where  $R$  (m/s) is the rainfall intensity;  $I$  (m/s) is the infiltration rate;  $h$  (m) is the cell water height (depth);  $z$  (m) is the cell topography elevation;  $u$  (m/s) and  $v$  (m/s) are the cell depth-averaged velocities in  $x$  and  $y$  directions, respectively;  $S_{fx}$  and  $S_{fy}$  are the cell friction slopes in  $x$  and  $y$  directions, respectively;  $g$  (m/s<sup>2</sup>) is gravity acceleration;  $t$  (s) is time.

The FullSWOF\_2D program fully solves SWEs on a structured mesh in two space dimensions using the finite volume method (FVM) which ensures mass conservation compared to the finite difference method (FDM) [34]. A well-balanced scheme was adapted to guarantee the positivity of water depth and the preservation of steady states for specific hydrological features such as during wet-dry transitions and tiny water depth [30,35]. Different boundary conditions, friction laws, and numerical schemes were developed which make the program a very powerful overland flow simulation software. The parallelization strategies of FullSWOF\_2D were also examined to improve its simulation efficiency dealing with large-scale cases [35]. A modified bi-layer (crust- and soil-layer) Green–Ampt (GA) infiltration model [36] to calculate  $I$  for Equation (1) was coupled in the FullSWOF\_2D [34] which enables the program to simulate overland flow on impervious and pervious surfaces.

FullSWOF\_2D has five boundary condition choices including the imposed discharge and water height case, wall condition, Neumann boundary (open boundary) condition, periodic variations of discharge and water height, and imposed discharge condition. It has three options of friction formulas including the Manning's equation, the Darcy–Weisbach equation, and the laminar law, as well as the no-friction setting. The simulation domain could be set nonuniformly by defining the friction value of every computational cell with an input file. The Rusanov flux, Harten–Lax–Van Leer (HLL) flux, Harten–Lax–Van Leer with Contact surface (HLLC) flux, HLL2, and HLLC2 [30] methods are provided to calculate every time level flux between computational cells. Three linear reconstruction methods include the MUSCL, ENO, and modified ENO, as well as three slope limiters, including the classical Minmod slope limiter, Van Albada limiter, and Van Leer's limiter, which are used in the reconstruction part of the 2nd order numerical scheme. The details about the numerical flux, reconstruction methods, and the limiters could be found in Bouchut's book [37].

The FullSWOF\_2D has been validated using several analytical solutions and benchmarks of the steady-state solutions and the transitory solutions. The steady-state solutions validated by FullSWOF\_2D include the emerged bump at rest and Mac Donald test cases with different settings.

The transitory solutions include the dam break on a dry domain and Thacker test case with a planar surface in paraboloid [38]. It is also widely used in the river flood simulation in a complex environment based on high-resolution topographic data [39] and spatial global sensitivity analysis of high-resolution classified topographic data in 2D urban flood modeling [40].

## 2.2. Particle Tracking Method (PTM) and FullSWOF-PTM

The PTM is a powerful method to study the characteristics of complex flow velocity fields during steady and transient state using simulated velocities from flow-governing equations, e.g., Equations (1)–(3) for shallow overland flow. It is widely used in different research areas, especially the groundwater flow and pollutant transport study [41]. Most of the commonly used PTMs provide satisfactory results for steady-state analysis [42]. PTMs could also be used for transient analysis under the assumption that the velocity field does not significantly change during the simulation duration. In Cheng's study [28], a PTM was developed based on the Lagrangian–Eulerian finite element method (FEM) which could reduce the numerical errors considerably and enable the PTM to trace fictitious particles in a complex flow field. It is suggested that the PTM could be extended to transient simulations by tracking velocity calculated with the velocity field of previous time levels and current time levels (stepwise approximation) when the FEM is used to solve the transport equations. Bensabat et al. [27] and Lu [43] developed a linear temporal interpolation scheme instead of a stepwise temporal approximation in order to count for the changes in velocity during a time step in complex unsteady flow while it is only suited to the FDM rather than FEM or FVM. The travel time and the pathlines could be generated using PTM directly incorporated with the overland flow simulation velocity field results.

In the previous study [29], the PTM using simulated velocities from DWM was developed to determine the travel time of different percentage particles' arrival at the outlet. The travel time of each particle in the simulation domain is computed using the PTM module that uses flow velocity fields simulated by the quasi-two-dimensional DWM at every time level. Over each time step, the particle travel distance is determined by the product of the appropriate tracking velocity (interpolated by the spatial linear method) and time step interval. In this study, a PTM module was incorporated with FullSWOF\_2D using a simulated velocity field at each time step, and the updated program became FullSWOF-PTM. A fourth-order Runge–Kutta (RK4) spatial interpolation scheme rather than linear spatial interpolation scheme [42] was adapted to get the particle velocity at each time step at different locations of the simulation domain. The temporal change of all particles was calculated and updated using the simulated particle velocity and time interval at every time step.

The following algorithm is implemented in the PTM code of FullSWOF-PTM at each time step: (1) The particle location is checked to determine whether it is within the simulation domain. If the particle arrives at the outlet cell, it is ignored and the tracking process moves on to the next particle. (2) The computational cell that the particle locates in and the adjacent cell for each particle are determined based on the particle location. (3) The particle velocities in  $x$ - and  $y$ -directions are spatially interpolated using a RK4 scheme based on the simulated  $x$  and  $y$  velocities of the cell that the particle locates in and adjacent computational cells at the time step. (4) The new locations of all particles are calculated and updated using previous locations, current particle velocities, and time step intervals. (5) The particle with the new location is checked again to determine whether it stays in the simulation domain or arrives at the outlet cell and gets out of the domain. (6) The percentage of particles remaining in the simulation domain is counted. The particle evolution information of each time step including the total number and percentage of particles remaining in the simulation domain is outputted during the whole simulation period with FullSWOF-PTM. A user interface for FullSWOF-PTM was developed using MATLAB r2017a (MathWorks, Natick, MA, United States) [44] to run all impervious and pervious cases in batches.

### 2.3. Modeling Cases

Three kinds of modeling cases were developed and simulated in this study: 11 testing cases, 446 impervious cases, and 750 pervious cases, and details are described below.

#### 2.3.1. FullSWOF-PTM Testing Cases

FullSWOF-PTM was validated using 11 rainfall events as testing cases to demonstrate that it can be used for accurate overland flow simulations. In Esteves's study [36], a 2D overland flow model solving SWEs based on an explicit FDM and coupled with the GA infiltration module was developed and calibrated/validated with the observed data on a natural hillslope plot. These observed rainfall and runoff data from 11 events plus the plot topography and soil infiltration data were obtained from Dr. Esteves and first used to test the FullSWOF-PTM model. The plot was 14.25 m long and 5 m wide, bordered by 150 mm wide cement blocks driven about 50 mm into the ground [45]. The cell size used in the simulation was 0.25 m based on a detailed topographic survey. The Darcy–Weisbach friction law (friction coefficient = 0.25) was used in the simulation. The plot was crusted, almost without vegetation. The infiltration model parameters including the saturated hydraulic conductivity ( $K$ , 0.0162 mm/h for crust and 77.4 mm/h for soil below), saturated water content ( $\theta_s$ , 0.245 for crust and 0.296 for soil), and suction head ( $\varphi$ ) of crust layer and soil, as well as the crust layer thickness (0.005 m) were all the same as the calibrated parameters used in Esteves's study [36].

The plot slope in  $x$ - and  $y$ -directions were  $0.0640 \pm 0.0292$  (from the right to left boundary) and  $0.0196 \pm 0.0155$  (from the top to bottom boundary), respectively. The right, top, and bottom boundaries of the study plot were all set as wall condition and the left (downstream) boundary was as Neumann (open) condition based on the field situation. The HLLC flux choice in FullSWOF-PTM was selected from the 1st order numerical scheme to calculate the new time level flux of each computational cell in the simulation. The Courant–Friedrichs–Lewy (CFL) condition (CFL = 0.4) was used to guarantee the numerical stability and calculate the time step interval for the simulation.

The rainfall data was measured with an electronic tipping-bucket recording rain gauge (each tip corresponding to 0.5 mm of rainfall). The discharge at the plot outlet was measured through a triangular  $20^\circ$  V-notch weir at every 5-second interval. The initial water content of the soil at the beginning of the rainfall was measured using a neutron-probe access tube located in the center of the plot [36]. The moisture deficit was calculated as the difference of saturation water content ( $\theta_s = \text{prosimy}$ ) and initial moisture content ( $\theta_i$ ).

The goodness of fit for the simulated hydrograph is evaluated using the Nash–Sutcliffe Efficiency (NSE) coefficient [46].

$$NSE = 1 - \frac{\sum_{j=1}^m (Q_{oj} - Q_{si})^2}{\sum_{j=1}^m (Q_{oj} - \bar{Q})^2} \quad (4)$$

where  $Q_{oj}$  ( $\text{m}^3/\text{s}$ ) is the  $j$ th observed runoff rate,  $Q_{sj}$  ( $\text{m}^3/\text{s}$ ) is the corresponding simulated runoff rate,  $\bar{Q}$  ( $\text{m}^3/\text{s}$ ) is the mean observed runoff rate, and  $m$  [-] is the total number of observed runoff rates. The NSE values for 11 rainfall events were calculated and compared with those reported by Esteves's program to evaluate the FullSWOF-PTM. The FullSWOF-PTM's performance was further evaluated by comparing simulated and observed runoff depth and peak discharge at the outlet.

#### 2.3.2. Impervious Modeling Cases

Using FullSWOF-PTM to model the overland flow on impervious surfaces has two purposes: (1) validating FullSWOF-PTM since calculated  $T_{ci}$  can be compared with many previous studies or established equations, and (2)  $T_{ci}$  will be used to develop  $T_{cp}$  equation. A total of 446 impervious modeling cases with different combinations of  $S_0$ ,  $n$ ,  $L$ , and  $i$  were simulated. In this study, the cell sizes in  $x$ - and  $y$ -directions and simulation domain width used for impervious and pervious modeling cases were 0.25, 0.25, and 1 m (4 cells in the  $y$ -direction, no cross slope), respectively. The Manning's

friction formula was selected among three friction formulas of FullSWOF-PTM. Figure 1 shows the model-parameter value distributions of the 446 cases, which also prove the parameter values are representative and set in the commonly used ranges [3].

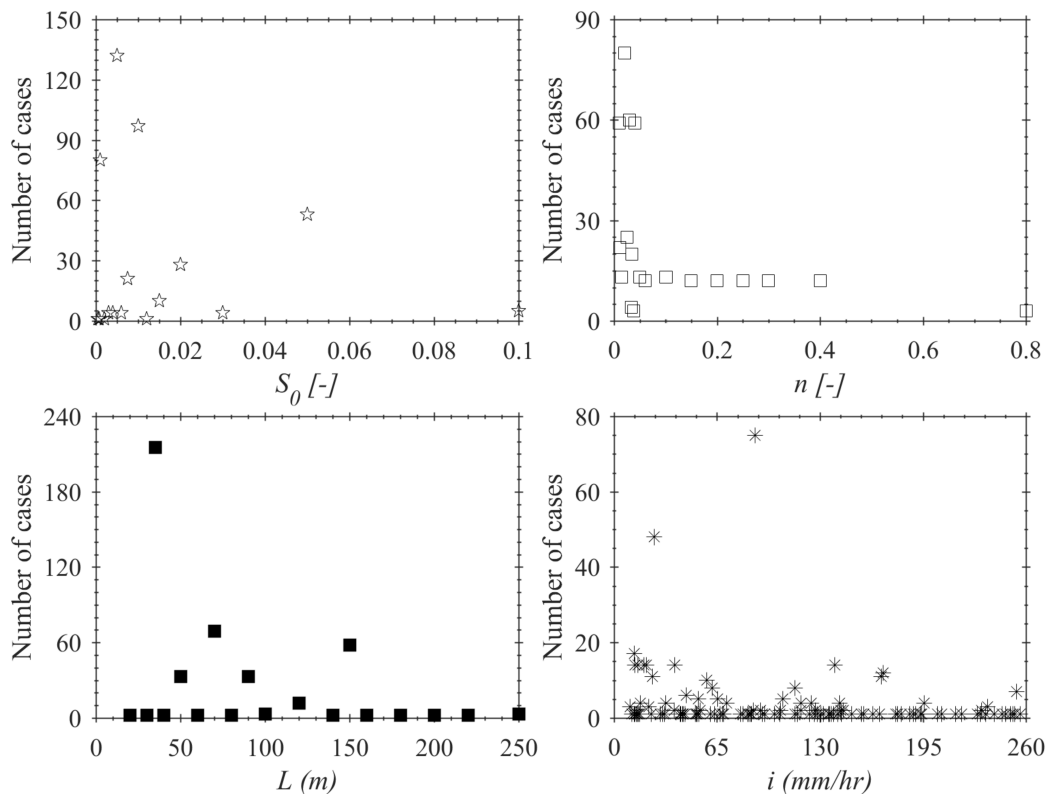


**Figure 1.** Distributions of the values of four model input parameters used for the 446 impervious modeling cases.

For 446 impervious modeling cases, the plot longitudinal slope  $S_0$  ranges from 0.0005 to 0.1 with the average slope of 0.0133 and standard deviation of 0.0175, and 86% of the cases have  $S_0 \leq 2\%$ . The Manning's roughness  $n$  ranges from 0.01 to 0.8 with 86% of  $n$  values less than 0.1. The plot length  $L$  ranges from 20 to 250 m; the rainfall intensity  $i$  ranges from 10.2 to 256.5 mm/h with the average value and standard deviation of 80.8 and 64.0 mm/h, respectively. There are 384 modeling cases with  $S_0 \leq 0.02$ , 395 cases with  $n \leq 0.15$ , 435 cases with  $L \leq 150$  m, and 381 cases with  $i \leq 150$  mm/h.

The topography file, rainfall file, particle initialization file, and model parameter file are required for FullSWOF-PTM in the impervious modeling cases, which were created using user-developed MATLAB code. The 2nd order numerical scheme in FullSWOF-PTM including the numerical flux methods (5 choices), linear reconstruction settings (3 choices), and slope limiters (3 choices) were tested using one impervious modeling case ( $S_0 = 0.05$ ,  $L = 35$  m,  $n = 0.01$ , and  $i = 12.7$  mm/h), which aims to identify the best numerical scheme among the 45 combinations. After performing the tests, all other impervious modeling cases were run in batches with MATLAB code using the tested best numerical scheme combination.

### 2.3.3. Pervious Modeling Cases

The GA infiltration parameters for different soil types of pervious surfaces were adapted from the research conducted by Rawls et al. [47]. The soil was categorized in this study into three groups: sand ( $K$  ranging from 25.4 to 127.0 mm/h), loam ( $K$  ranging from 2.54 to 12.7 mm/h), and clay ( $K$  ranging from 0.23 to 1.52 mm/h) groups depending upon the saturated hydraulic conductivity. There were 204,

350, and 196 modeling cases for sand, loam, and clay soil, respectively. A total of 750 modeling cases were developed and simulated while one  $T_{cp}$  equation was derived from the results of all pervious surfaces rather than developing three equations for different soil groups. The crust thickness of the pervious plots is set equal to zero because this study focused on the influence of soil property on the  $T_{cp}$  for pervious surfaces. The soil infiltration parameters (saturated hydraulic conductivity  $K$ , suction head  $\varphi$ , and moisture deficit  $\Delta\theta$ ) used for the 750 modeling cases are shown in Figure 2. A dimensionless saturated hydraulic conductivity  $K'$  ( $=K/i$ ), which was used by Akan in the derivation of the  $T_{cp}$  equation for pervious surfaces [24], was calculated and ranged from 0.001 to 0.97 for the 750 modeling cases (Figure 2). Since  $K'$  is less than 1, it means  $K < i$  and all pervious modeling cases should produce runoff eventually when the rainfall duration is long enough. Equation (5) developed by Akan [24] is limited to  $K' \leq 0.4$ , i.e.,  $i \geq 2.5 K$ , which means Akan's equation does not apply to relatively small rainfall intensity in comparison to  $K$ , but in reality  $i$  can be larger or even smaller than  $K$ . When  $i \leq K$ , it is not applicable to determine the  $T_{cp}$  for pervious surfaces since there is no surface runoff as all rainfall is infiltrated.

$$T_{cp\_A} = \left(\frac{Ln}{\sqrt{S_0}}\right)^{0.60} \frac{1}{(i - K)^{0.40}} + 3.1 \frac{K^{1.33} \varphi \Delta\theta}{i^{2.33}} \quad (\text{For } K' \leq 0.4) \quad (5)$$

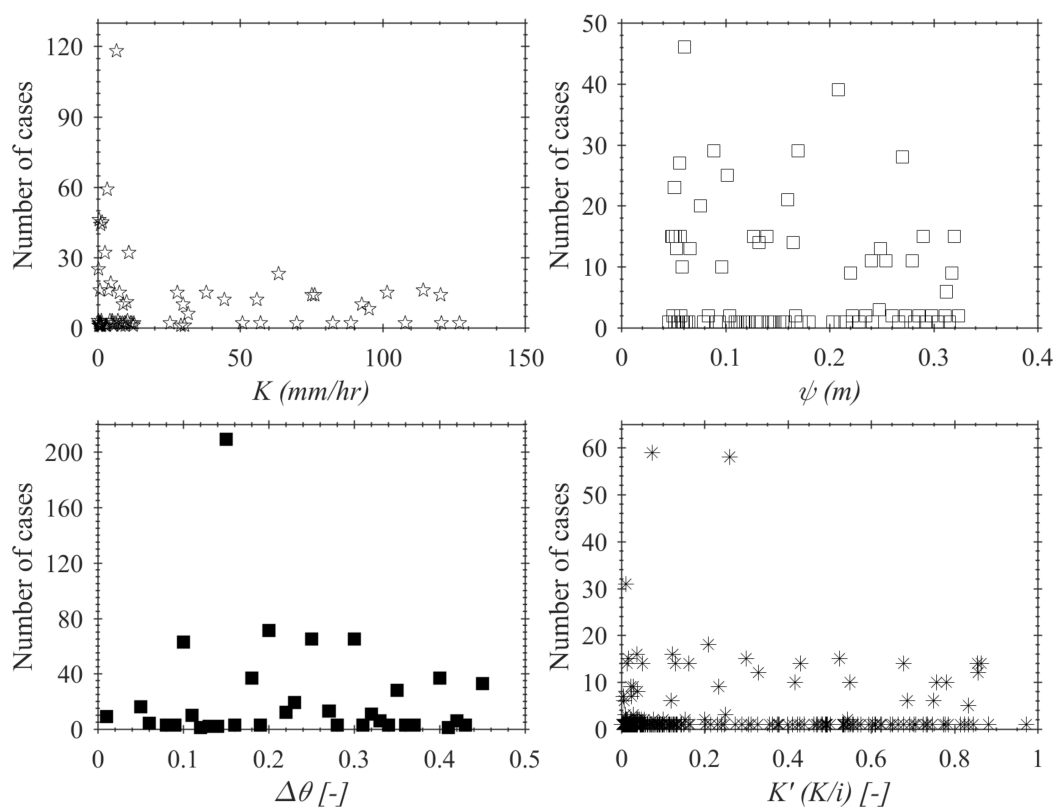


**Figure 2.** Distributions of the values of three soil infiltration parameters and calculated  $K' = K/i$  used for 750 pervious modeling cases.

The representative values of infiltration parameters of three soil groups were selected from literature [47] for 750 modeling cases. The saturation hydraulic conductivity ranges from 0.23 to 127 mm/h. The soil dry suction head ranges from 0.0457 to 0.3238 m. The moisture deficit ranges from 0.01 to 0.45.

### 3. Results and Discussion

#### 3.1. FullSWOF-PTM Testing Results

The simulated discharges from FullSWOF-PTM were divided by the drainage area and compared to the observed runoff data (mm/h) for all 11 testing events. The comparison of observed and simulated discharge hydrographs on 24 August and 4 September, 1994, are shown in Figure 3 as sample results, and the hydrographs closely follow rainfall variations. It shows that the FullSWOF-PTM simulation results have strong consistency with the observed data during the whole rainfall period.

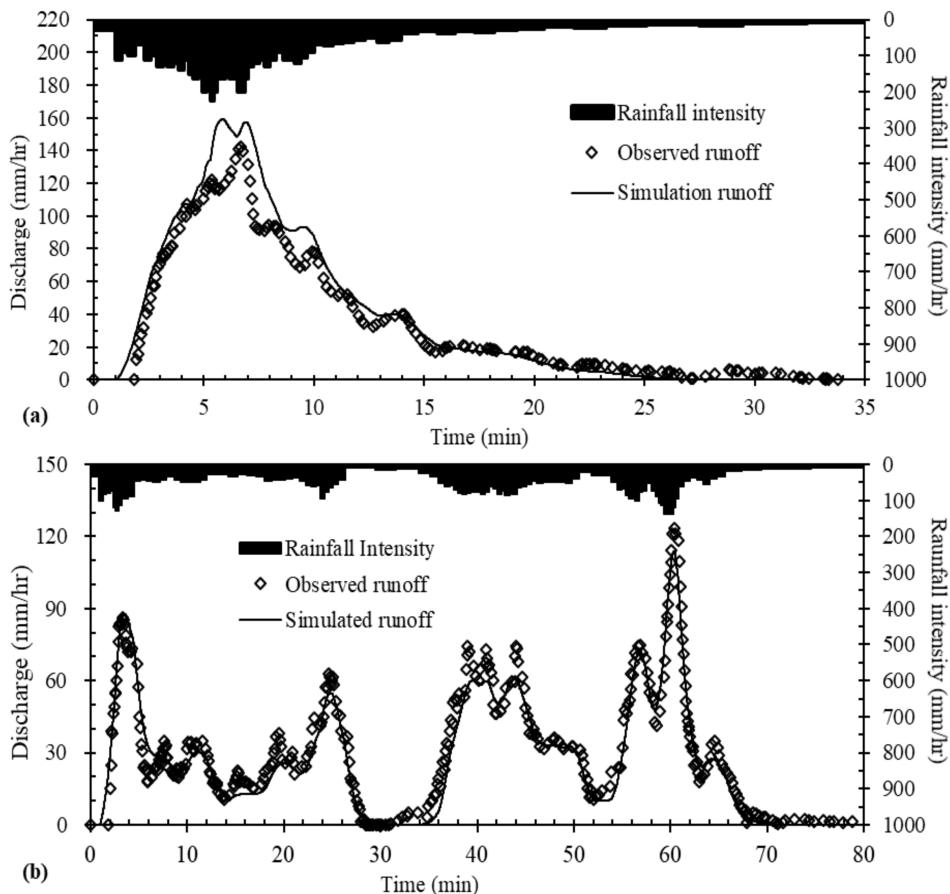


**Figure 3.** Comparison of simulated and observed hydrographs of two events on (a) 24 August and (b) 4 September, 1994.

For 11 rainfall events, the initial moisture content  $\theta_i$  ranged from 0.048 to 0.106 (Table 1). Since the soil porosity of the field was 0.296, the moisture deficit  $\Delta\theta$  ranged from 0.190 to 0.248. The discharge NSE values of FullSWOF-PTM and Esteves's programs ranged from 0.64 to 0.95 (average  $\pm$  standard deviation as  $0.75 \pm 0.11$ ) and from 0.46 to 0.93 ( $0.79 \pm 0.15$ ), respectively; and this indicates FullSWOF-PTM performed as well as Esteves's program in simulating overland flows. Table 1 also gives the comparison of simulated and observed runoff depths (mm) and peak discharges (mm/h). The percent errors of simulated runoff depths and peak discharges are  $1.9\% \pm 15.9\%$  (average  $\pm$  standard deviation) and  $-4.4\% \pm 16.3\%$ , respectively. The results for all 11 rainfall events (Table 1 and Figure 3) show that the FullSWOF-PTM program predicts the rainfall–runoff process of overland flows on a pervious surface with reasonable accuracy.

**Table 1.** Comparison of simulated and observed discharge parameters for 11 rainfall events.

Events [ $\theta_i, R_D$ ]	NSE <sup>1</sup>	NSE <sup>2</sup>	D <sub>ob</sub> <sup>2</sup> (mm)	D <sub>si</sub> <sup>1</sup> (mm)	$\Delta D$ (%)	Q <sub>po</sub> <sup>2</sup> (mm/h)	Q <sub>ps</sub> <sup>1</sup> (mm/h)	$\Delta Q_p$ (%)
Jul 20 [0.048, 51.5]	0.81	0.85	29.0	32.4	11.7	144.5	165.5	14.5
Jul 21 [0.103, 59.5]	0.68	0.66	26.7	30.1	12.7	77.0	85.2	10.6
Aug 7 [0.100, 30.0]	0.71	0.90	22.0	20.8	-5.5	179.4	138.3	-22.9
Aug 10 [0.106, 11.0]	0.75	0.90	5.6	5.6	0.0	59.1	52.4	-11.3
Aug 20 (1) [0.067, 22.0]	0.69	0.63	9.7	7.2	-25.8	42.0	33.1	-21.2
Aug 20 (2) [0.095, 4.0]	0.70	0.90	2.2	1.7	-22.7	50.5	37.0	-26.7
Aug 24 [0.088, 31.0]	0.90	0.88	18.8	21.0	11.7	142.2	159.0	11.8
Aug 25 [0.085, 24.0]	0.82	0.89	14.3	14.3	0.0	91.6	86.7	-5.3
Sep 4 [0.082, 62.0]	0.95	0.93	37.8	35.1	-7.1	123.5	113.7	-7.9
Sep 8 [0.082, 31.0]	0.62	0.46	15.3	20.4	33.3	86.7	107.3	23.8
Sep 16 [0.061, 9.5]	0.60	0.66	2.4	2.7	12.5	48.4	41.8	-13.6

Note:  $\theta_i$  is initial soil moisture content,  $R_D$  is rainfall depth in mm, <sup>1</sup> is calculated using FullSWOF-PTM simulated and observed data, <sup>2</sup> is adapted from Esteves’s paper after comparing with observed data [36], D<sub>ob</sub> (mm) is the observed total runoff depth, D<sub>si</sub> (mm) is the simulated total runoff depth,  $\Delta D$  (%) is the percent error of simulated runoff depth =  $(D_{si} - D_{ob})/D_{ob} \times 100\%$ , Q<sub>po</sub> (mm/h) is the observed peak runoff rate, Q<sub>ps</sub> (mm/h) is the simulated peak runoff rate,  $\Delta Q_p$  (%) is the percent error of simulated peak discharge =  $(Q_{ps} - Q_{po})/Q_{po} \times 100\%$ .

### 3.2. Time of Concentration ( $T_{ci}$ ) of Impervious Surfaces

In previous studies [2,7,9,15,48],  $T_c$  was evaluated as the time when discharge at the outlet reaches a specific percentage of the equilibrium discharge, e.g., 90%, 95%, or 98% of peak discharge ( $Q_p$ ). However, it is difficult to evaluate  $T_c$  for pervious surfaces using the fixed percent  $Q_p$  because there is almost no equilibrium discharge for pervious surfaces. In this study, the travel time for 85% of particles arriving at the drainage outlet ( $T_{r-p85}$ ) was used to evaluate the  $T_c$  for both impervious and pervious surfaces based on the previous PTM studies [29].

Figure 4 shows simulated outlet discharge and the in-domain particle percentage versus time under eight Manning’s roughness coefficients but the same plot slope, length, and rainfall intensity. The 2nd order numerical scheme combinations HLL2 for the numerical flux, ENO for the linear reconstruction, and Vanleer for the slope limiter [37] were used for the simulation because the simulated  $Q_p$  was exactly the same as  $Q_p$  calculated by the rational method and the run time for the program is the shortest. Simulated discharges verses time by FullSWOF-PTM give S-hydrographs [49] in Figure 4 under the constant rainfall intensities over a long period of time. The outlet discharge increases and the in-domain particle percentage decreases as the constant rainfall continues, and finally both reach the equilibriums. Based on the rational equation, the peak discharge ( $Q_{pr}$ ) for all eight runs should be the same and equal to 0.864 L/s, which is the same as FullSWOF-PTM simulated  $Q_p$  (Figure 4).

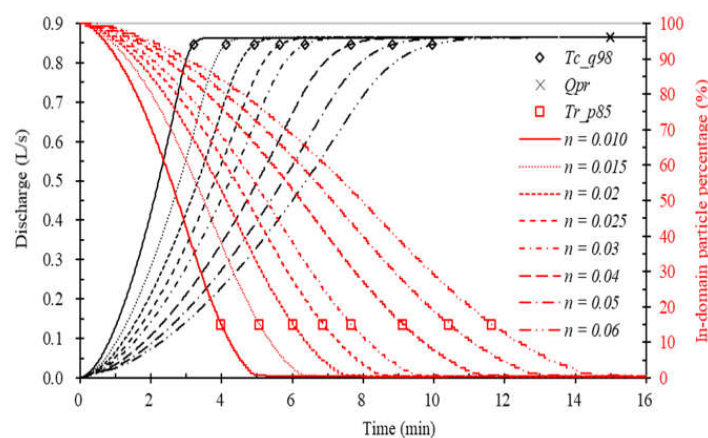


**Figure 4.** Simulated outlet discharge and in-domain particle percentage versus time under different roughness ( $n$ ) coefficients for eight modeling cases with  $i = 88.9$  mm/h,  $S_0 = 0.005$ , and  $L = 35$  m of impervious surfaces.

On Figure 4,  $T_{c_{q98}}$  is the  $T_c$  defined or calculated as the travel time when the runoff reaches the 98% percent of the equilibrium discharge  $Q_{pr}$ , and  $T_{r_{p85}}$  is the travel time when the in-domain particle percentage is 15%. Both  $T_{c_{q98}}$  and  $T_{r_{p85}}$  increase with the increase of the roughness (Figure 4) since the flow velocity is smaller with higher roughness. Figure 4 indicates that  $T_{c_{q98}}$  is somewhat smaller than  $T_{r_{p85}}$  for each case, which is the same as the conclusion of the previous research [29].

A generalized power relation, Equation (6) was chosen to develop the regression equation for  $T_{ci}$  as a function of four input/influencing parameters ( $L$ ,  $n$ ,  $S_0$ , and  $i$ ). The three influencing parameters  $L$ ,  $n$ , and  $S_0$  that describe/characterize the overland flow surface were grouped as a combined parameter ( $Ln/\sqrt{S_0}$ ) because the Manning’s equation was used in FullSWOF-PTM as friction formula for the overland flow resistance [24]. The  $T_{r_{p85}}$  obtained from FullSWOF-PTM was considered as  $T_{ci}$  or  $T_{ci_{p85}}$  (Figure 5), and  $T_{r_{p85}}$  values for all 446 impervious modeling cases were used to develop the  $T_{ci}$  regression equation.

$$T_{ci} = \left(\frac{Ln}{\sqrt{S_0}}\right)^{k_1} \frac{1}{i^{k_2}} \tag{6}$$

The exponents ( $k_1$  and  $k_2$ ) were estimated using the MLR method after the log transformation of Equation (6), and the resulting regression equations of  $T_{ci_{p85}}$  are:

$$T_{ci} = \left(\frac{nL}{\sqrt{S_0}}\right)^{0.608} \frac{1}{i^{0.422}} \quad (R^2 = 0.996) \tag{7}$$

$$T_{ci} = 9.741 \times \left(\frac{nL}{\sqrt{S_0}}\right)^{0.608} \frac{1}{i^{0.422}} \tag{8}$$

where  $L$  is in (m),  $n$  is in [-],  $S_0$  is in [-],  $T_{ci}$  of Equation (7) is in seconds and Equation (8) in minutes, respectively, when  $i$  for Equation (7) is in m/s and for Equation (8) in mm/h. FullSWOF-PTM uses  $i$  in m/s for all computations (1 m/s = 3,600,000 mm/h). The 95% confidence intervals for  $k_1$  and  $k_2$  are [0.606, 0.610] and [0.421, 0.423] with  $p$ -value < 0.0001, respectively. The average difference between  $T_{ci}$  calculated using Equation (7) and simulated  $T_{ci_{p85}}$  is 0.11 min with a standard deviation of 1.45 min (Figure 5).

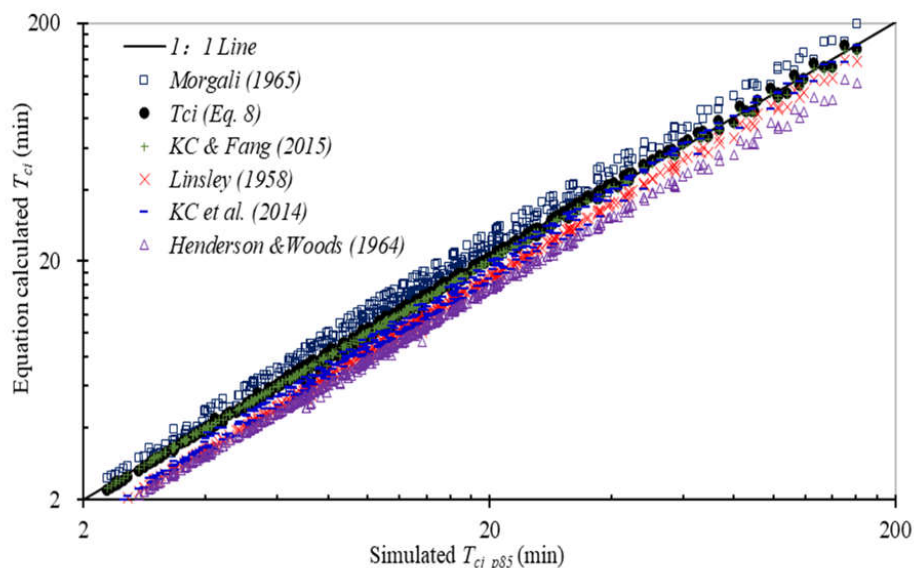


**Figure 5.**  $T_{ci}$  calculated from six equations (Table 2) versus simulated  $T_{ci_{p85}}$  for 446 modeling cases of impervious surfaces.

**Table 2.** Six  $T_{ci}$  equations and statistical results when compared with simulated  $T_{ci\_p85}$  (Figure 5).

Source	$T_{ci}$ Formula (min)	$R^2$	RMSE (min)
$T_{ci}$ (Equation (8))	$T_{ci} = 9.741 \times (nL/\sqrt{S_0})^{0.608} / i^{0.422}$	0.996 ( $1.00 \times T_{ci\_p85}$ ) <sup>1</sup>	1.45
Linsley (1958)	$T_{ci} = 6.82(nL/\sqrt{S_0})^{0.633} / i^{0.398}$	0.998 ( $0.87 \times T_{ci\_p85}$ )	4.15
Henderson & Woods (1964)	$T_{ci} = 6.98(nL/\sqrt{S_0})^{0.60} / i^{0.40}$	0.997 ( $0.74 \times T_{ci\_p85}$ )	8.04
Morgali (1965)	$T_{ci} = 7.05L^{0.593}n^{0.605} / (i^{0.388}S_0^{0.38})$	0.995 ( $1.19 \times T_{ci\_p85}$ )	6.08
KC et al., (2014)	$T_{ci} = 8.67 \times L^{0.541}n^{0.649} / (i^{0.391}S_0^{0.359})$	0.994 ( $0.96 \times T_{ci\_p85}$ )	2.33
KC & Fang (2015)	$T_{ci} = 9.25 \times L^{0.599}n^{0.609} / (i^{0.399}S_0^{0.303})$	0.997 ( $0.98 \times T_{ci\_p85}$ )	1.38

Note: <sup>1</sup>—the fitted equation between each equation-calculated  $T_{ci}$  and  $T_{ci\_p85}$  is given inside brackets after  $R^2$ .

Figure 5 shows calculated  $T_{ci}$  from Equation (8) and five other equations [50–54] versus simulated  $T_{ci\_p85}$ . The calculated  $T_{ci}$  from all six equations (Table 2) linearly correlates well with the simulated  $T_{ci\_p85}$  as indicated by  $R^2 > 0.994$  and regression equations in Table 2. This proves Equation (8) developed from  $T_{ci\_p85}$  predicts well  $T_c$  for impervious surfaces and the travel time for 85% of particles to arrive at the outlet can be considered as  $T_{ci}$  with reasonable accuracy. The root-mean-square error (RMSE) value of the KC and Fang's equation (2015), also based on the travel time for 85% of particles to arrive at the outlet [29], is the smallest (1.38 min, Table 2) and the RMSE of Equation (8) is just slightly larger. In overall, the Henderson & Woods and Linsley equations underestimate  $T_{ci\_p85}$  while the Morgali equation overestimates, and the remaining three equations predict  $T_{ci}$  well with lower RMSE for impervious surfaces.

### 3.3. Time of Concentration ( $T_{cp}$ ) of Pervious Surfaces

The responding runoff hydrographs and in-domain particle percentages of eight saturation hydraulic conductivity values for pervious surfaces ( $S_0 = 0.01$ ,  $L = 50$  m,  $\varphi = 0.06$  m,  $\Delta\theta = 0.18$ ) are summarized and compared in Figure 6 under constant rainfall intensity ( $i = 105.2$  mm/h). Figure 6 clearly indicates that the PTM is the only choice to evaluate  $T_{cp}$  for pervious surfaces because it is not practical to run the simulation for very long periods for the runoff to reach acceptable equilibrium. For a pervious surface, the rainfall in the early period will completely infiltrate when the rainfall intensity is smaller than the infiltration capacity [55] (Figure 6). The time prior to ponding or the start of surface runoff is defined as the ponding time, which depends on both the rainfall intensity and infiltration rate. When the Green–Ampt infiltration model is used, the ponding time ( $t_p$ ) under constant rainfall intensity is calculated using Equation (9) [56].

$$t_p = \frac{\varphi\Delta\theta K}{i(i-K)} = \frac{\varphi\Delta\theta K'}{i(1-K')} \quad (9)$$

For eight modeling cases on Figure 6,  $K$  ranges from  $7.06 \times 10^{-6}$  to  $19.4 \times 10^{-6}$  m/s (25.4–69.8 mm/h), which belongs to sandy loam or sand soil groups, and the ponding time from Equation (9) ranges from 1.96 to 12.2 min, which is the same as predicted by FullSWOF-PTM. Equation (9) is valid when  $i > K$ , but if  $t \leq t_p$  even when  $i > K$ , there is still no surface runoff and then it is not necessary and not meaningful to determine  $T_{cp}$  for pervious surfaces. For impervious surfaces,  $T_{ci}$  always exists for any non-zero rainfall intensity (Table 2).

For pervious surfaces, the outlet discharge decreases with the increase of  $K$  (Figure 6) because of more infiltration. The outlet discharge and in-domain particle percentage are postponed more and more when  $K$  and the soil infiltration capacity increases. The in-domain particle percentage is 100% when  $t \leq t_p$ . The travel time for 85% of particles to arrive at the outlet  $T_{r\_p85}$  was calculated by FullSWOF-PTM from the beginning of the rainfall event and ranges from 10.7 to 27.8 min (open squares on Figure 6) for these eight cases.

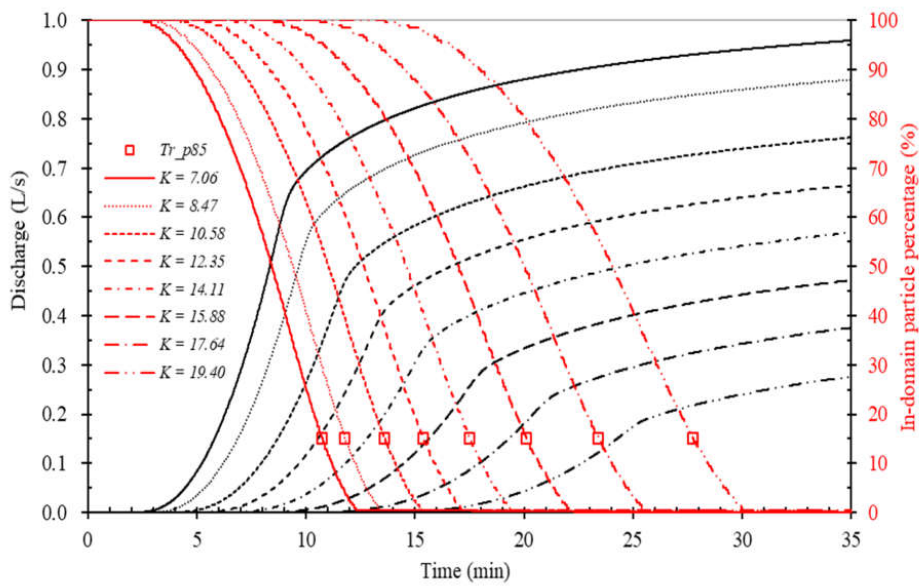


**Figure 6.** Simulated runoff hydrograph and in-domain particle percentage versus time for eight modeling cases of different saturation hydraulic conductivity ( $K$ , in  $10^{-6}$  m/s) with  $S_0 = 0.01$ ,  $i = 105.2$  mm/h,  $L = 50$  m,  $\varphi = 0.06$  m,  $\Delta\theta = 0.18$  of pervious surfaces.

In this paper, the time of concentration for a pervious surface  $T_{cp}$  is considered as  $T_{r\_p85}$  of pervious surfaces determined from FullSWOF-PTM minus the ponding time  $t_p$  determined using Equation (9), and presented in Equation (10). Figure 7 plots cumulative distributions of  $t_p$  calculated from Equation (9), simulated  $T_{r\_p85}$ , and  $T_{cp}$  for all 750 modeling cases, and their statistical summary is given in Table 3. The modeling cases with large  $t_p$  and  $T_{r\_p85}$  have small differences between  $i$  and  $K$ . For 750 cases,  $t_p$  is 0.2% to 82.6% of  $T_{r\_p85}$ , and 50% of  $t_p$  is less than 18.8% of  $T_{r\_p85}$ . Excluding  $t_p$  from  $T_{r\_p85}$ , it means  $T_{cp}$  is not counted from the beginning of the rainfall but the commencing of the runoff, and this is consistent with Guo’s study [4]. The purpose of subtracting  $t_p$  from  $T_{r\_p85}$  is also to advise engineers and designers that it is not meaningful to determine  $T_{cp}$  for pervious surfaces when the rainfall duration is less than  $t_p$ . It is recommended that  $t_p$  should be calculated, e.g., using Equation (9), before  $T_{cp}$  for a pervious surface is calculated.

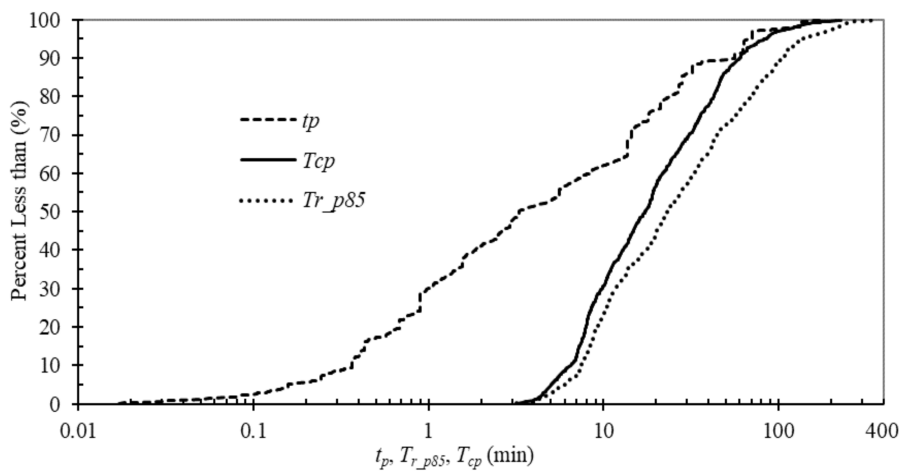


**Figure 7.** Cumulative distributions of calculated ponding time  $t_p$  from Equation (9), time of 85% of particles to arrive at the outlet  $T_{r\_p85}$ , and time of concentration  $T_{cp}$  of pervious surfaces for 750 modeling cases.

**Table 3.** Statistical summary of  $t_p$ ,  $T_{r,p85}$ , and  $T_{cp}$  of pervious surfaces for 750 modeling cases.

Parameter	$t_p$ (min)	$T_{r,p85}$ (min)	$T_{cp}$ (min)
Minimum	0.02	3.2	3.2
50 percentiles	3.3	23.2	17.3
75 percentiles	18.0	56.6	35.8
90 percentiles	56.0	104.7	60.3
95 percentiles	69.1	136.3	82.6
Maximum	180.1	351.6	227.8

Note:  $t_p$  is the ponding time,  $T_{r,p85}$  is the travel time for 85% of particles to arrive at the outlet from the beginning of rainfall, and  $T_{cp}$  is the time of concentration for pervious surfaces, which is equal to  $T_{r,p85} - t_p$ .

Following Akan’s study [24],  $T_{cp}$  is considered as the sum of the time of concentration of an equivalent impervious surface ( $T_{ci}$ ) using  $(i - K)$  as effective rainfall and additional travel time due to infiltration ( $T_{rs}$ ) related to the soil infiltration properties. A generalized power relation in Equation (10) was used to develop a regression equation for  $T_{rs}$  and then for  $T_{cp}$  equation of pervious surfaces based on the simulated  $T_{r,p85}$  of 750 pervious modeling cases.

$$T_{cp} = T_{r,p85} - t_p = T_{ci} + T_{rs} = \left(\frac{Ln}{\sqrt{S_0}}\right)^{0.608} \frac{1}{(i - K)^{0.422}} + c_1 \frac{K^{c_2} \varphi^{c_3} \Delta\theta^{c_4}}{i^{c_5}} \tag{10}$$

The exponents ( $C_1, C_2, C_3, C_4,$  and  $C_5$ ) in Equation (10) were determined using the MLR regression between  $y = T_{r,p85} - t_p - T_{ci}$  and  $x = (K, \varphi, \Delta\theta,$  and  $i)$  after log-transformed. The fit results of five exponents were summarized in Table 4 and Equation (11).

$$T_{cp} = \left(\frac{Ln}{\sqrt{S_0}}\right)^{0.608} \frac{1}{(i - K)^{0.422}} + 2.162 \frac{K^{0.535} \varphi^{0.161} \Delta\theta^{0.645}}{i^{1.213}} \tag{11}$$

where  $T_{cp}$  is in seconds when  $L$  is in m;  $n, S_0,$  and  $\Delta\theta$  are dimensionless,  $i$  and  $K$  are in m/s, and  $\varphi$  in m. The regression equation for  $T_{cp}$  has a  $p$ -value  $< 0.0001$ , and the residuals between calculated  $T_{cp}$  from Equation (11) and  $T_{r,p85} - t_p$  range from  $-15.4$  to  $53.3$  min with average residual of  $1.12$  min (standard deviation  $6.13$  min). One can see that Equation (11) developed from this study can be used to determine  $T_c$  of overland flows for both impervious (setting  $K = 0$ ) and pervious surfaces.

**Table 4.** MLR fitted exponents  $C_1$  to  $C_5$  of Equation (10) and corresponding 95% confidence intervals.

Parameter	Value	95% Confidence Interval
$C_1$	2.162	[0.875, 5.340]
$C_2$	0.535	[0.488, 0.582]
$C_3$	0.161	[0.030, 0.292]
$C_4$	0.645	[0.591, 0.699]
$C_5$	1.213	[1.172, 1.255]

The comparison of Equation (11) and Akan’s Equation (5) was shown in Figure 8: (a) for  $K' \leq 0.4$  (427 modeling cases) and (b) for all 750 modeling cases since Akan [24] developed Equation (5) for  $K' \leq 0.4$ . Akan’s time of concentration for pervious surfaces ( $T_{cp\_A}$ ) is counted from the beginning of the rainfall event and includes the period before the ponding time; therefore,  $T_{cp}$  from Equation (11) and  $T_{cp\_A} - t_p$  are plotted against  $T_{r,p85} - t_p$  on Figure 8. Akan’s  $T_{cp\_A} - t_p$  is linearly correlated well with  $T_{r,p85} - t_p$  when the overall  $R^2$  is 0.992, but underestimated since  $T_{cp\_A} - t_p = 0.664 (T_{r,p85} - t_p)$  (Figure 8) and RMSE is 13.7 min. The RMSEs of Equation (11) is 4.8 min and the overall  $R^2$  are 0.993.

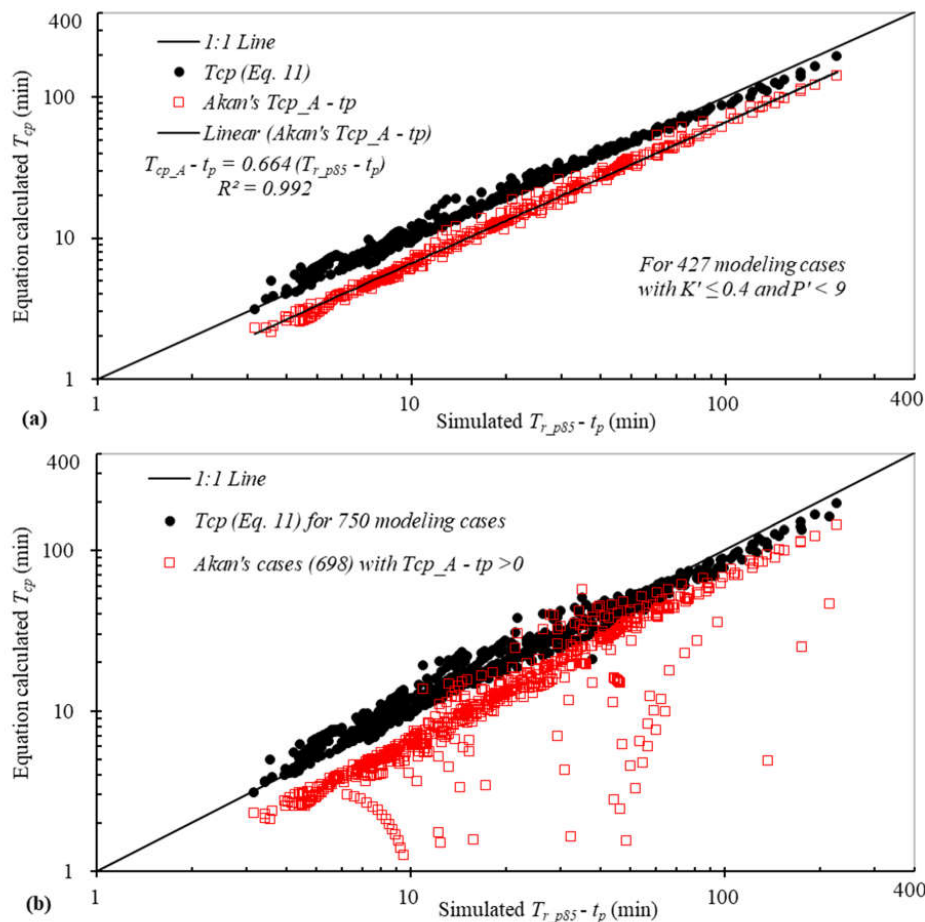


**Figure 8.** Comparison of equation calculated  $T_{cp}$  and  $T_{r\_p85} - t_p$ : (a) 427 modeling cases with  $K' \leq 0.4$  and  $P' < 9$  cases, (b) 750 modeling cases for Equation (11) and 698 modeling cases with Akan's  $T_{cp} - t_p > 0$ .

Figure 8b shows the comparison of calculated  $T_{cp}$  from Equation (11) for 750 modeling cases and  $T_{cp\_A} - t_p$  for 698 cases with  $T_{cp\_A} - t_p > 0$  against  $T_{r\_p85} - t_p$ . When Akan's Equation (5) is applied to 323 modeling cases with  $K' > 0.4$ , there are 52 cases having  $T_{cp\_A} - t_p < 0$  or  $T_{cp\_A} < t_p$ , which were not shown on the log scale plot (Figure 8). The  $R^2$  of Equation (11) and Akan's  $T_{cp\_A} - t_p$  are 0.979 for 750 cases and 0.792 for 698 cases with  $T_{cp\_A} - t_p > 0$ , respectively. The RMSE of Equation (11) and Akan's  $T_{cp\_A} - t_p$  are 6.2 min and 18.0 min, respectively. Figure 8 and the above analysis show Akan's Equation (5) should not be applied to beyond its limits:  $K' \leq 0.4$  and  $P' < 9$ , where  $P' = \varphi\Delta\theta/iT_{ci}$  and  $T_{ci}$  used by Akan in Equation (5) is the same as Henderson and Woods'  $T_{ci}$  equation [24]. Akan introduced  $P'$  for solving non-dimensional flow and infiltration equations but did not explain any physical meaning of  $P'$  [10,19,24]. One can see that  $iT_{ci}$  is rainfall depth over  $T_{ci}$  of impervious surface of the same geometry and the ponding time increases with  $\varphi\Delta\theta$  indicated by Equation (9). Akan [24] indicated  $K' \leq 0.4$  and  $P' < 9$  are for most practical applications without providing any reason. For 750 modeling cases studied here, the limits of  $K'$  values are [0.001, 0.97] and of  $P'$  values are [0.18, 55.27]. Therefore, Equation (11) developed from this study can be used to estimate  $T_{cp}$  for pervious surfaces with reasonable accuracy and over wide ranges of input parameters, especially for small rainfall intensities in comparison to  $K$ .

#### 4. Summary and Conclusions

The particle tracking method (PTM) module was added into the 2D overland flow simulation program based on the open-source program FullSWOF\_2D that can be used to estimate the time

of concentration for impervious and pervious surfaces. The FullSWOF-PTM program was tested using published rainfall and runoff data and simulated hydrographs match well with observed data (Table 1), which proves it can predict the overland flow accurately. Four hundred and forty-six impervious modeling cases were developed and simulated to explore  $T_{ci}$  of overland flow on impervious surfaces. The travel time of 85% of particles to arrive at the drainage outlet ( $T_{r_{p85}}$ ) was calculated by FullSWOF-PTM for determining the time of concentration of impervious and pervious surfaces in this study. A regression equation of  $T_{ci}$ , Equation (7) was derived using the MLR regression method and as a power function of  $Ln/\sqrt{S_0}$  and  $i$ . The derived impervious surface  $T_{ci}$  equation matches well with  $T_{r_{p85}}$  and correlates well with  $T_{ci}$  from other five published equations, which further proves FullSWOF-PTM can be used to estimate  $T_{cp}$  of overland flow on pervious surfaces.

Seven hundred and fifty pervious modeling cases were developed and simulated to explore the  $T_{cp}$  equation. In this study,  $T_{cp}$  is considered as  $T_{r_{p85}}$  of pervious surfaces determined from FullSWOF-PTM minus the ponding time  $t_p$  determined using Equation (9). It means  $T_{cp}$  is not counted from the beginning of the rainfall but the commencing of the runoff. Engineers and designers should calculate  $t_p$  first, e.g., using Equation (9), before  $T_{cp}$  for pervious surface is calculated because it is not meaningful to determine  $T_{cp}$  for pervious surfaces when the rainfall duration is less than  $t_p$ . A regression equation for  $T_{cp}$ , Equation (11) was developed using simulated  $T_{r_{p_{p85}}}$  and calculated  $t_p$  from 750 pervious modeling cases. Equation (11) includes  $T_{ci}$  for an equivalent impervious surface using  $(i - K)$  as effective rainfall and additional travel time due to infiltration ( $T_{rs}$ ) as a function of rainfall intensity and the soil infiltration parameters ( $K$ ,  $\phi$ , and  $\Delta\theta$ ). Therefore, Equation (11) can be used for both impervious and pervious surfaces. The derived  $T_{cp}$  equation has higher  $R^2$  and smaller RMSE compared to Akan's equation as well as wide ranges of input parameters.

**Acknowledgments:** The research was partially supported by the National Natural Science Foundation of China (No. 51478026), Beijing Higher Education High Level Teachers Team Construction Program (CIT&TCD 201704055) and Beijing University of Civil Engineering and Architecture Research Fund for Pyramid Talents Development. The author, Xiaoning Li, wishes to express his gratitude to the Chinese Scholarship Council for financial support pursuing his graduate study at Auburn University.

**Author Contributions:** Xiaoning Li added the PTM code into FullSWOF\_2D program, conducted the model runs and result analysis, and prepared the manuscript draft. Xing Fang supervised model development, simulation runs, and data analysis, and revised the manuscript. Manoj KC collected the basic simulation data and revised the manuscript. Junqi Li, Yongwei Gong, and Gang Chen supervised the writing and data analysis, and revised the manuscript. All authors made contributions to the study and writing the manuscript.

**Conflicts of Interest:** The authors declare no conflict of interest.

## References

1. Mulvany, T.J. On the use of self-registering rain and flood gauges in making observations of the relations of rainfall and flood discharges in a given catchment. *Proc. Inst. Civil Eng. Irel.* **1851**, *4*, 18–33.
2. Kuichling, E. The relation between the rainfall and the discharge of sewers in populous areas. *Trans. Am. Soc. Civ. Eng.* **1889**, *20*, 1–56.
3. Brown, S.; Stein, S.; Warner, J. *Urban Drainage Design Manual: Hydraulic Engineering Circular No. 22*; FHWA-NHI-10-009 HEC-22; National Highway Institute: Fort Collins, CO, USA, 2009.
4. Guo, J.C.Y. Overland flow on a pervious surface. *Water Int.* **1998**, *23*, 91–96. [[CrossRef](#)]
5. Kibler, D.F. Desk-top methods for urban stormwater calculation. *Urban Stormwater Hydrol.* **1982**, 87–135. [[CrossRef](#)]
6. McCuen, R.H.; Wong, S.L.; Rawls, W.J. Estimating urban time of concentration. *J. Hydraul. Eng.* **1984**, *110*, 887–904. [[CrossRef](#)]
7. Izzard, C.F. Hydraulics of runoff from developed surfaces. In *Proceedings of the 26th Annual Meetings of the Highway Research Board, Washington, DC, USA, 5–8 December 1946*; Crum, R.W., Burggraf, F., William, N.C., Jr., Eds.; Highway Research Board: Washington, DC, USA, 1946; pp. 129–150.
8. Muzik, I. Laboratory experiments with surface runoff. *J. Hydraul. Div.* **1974**, *100*, 501–516.
9. Wong, T.S.W. Assessment of time of concentration formulas for overland flow. *J. Irrig. Drain. Eng.* **2005**, *131*, 383–387. [[CrossRef](#)]

10. Akan, A.O. Time of concentration of overland flow. *J. Irrig. Drain. Eng.* **1986**, *112*, 283–292. [[CrossRef](#)]
11. Wooding, R.A. A hydraulic model for the catchment-stream problem: I. Kinematic-wave theory. *J. Hydrol.* **1965**, *3*, 254–267. [[CrossRef](#)]
12. Woolhiser, D.A.; Liggett, J.A. Unsteady, one-dimensional flow over a plane—The rising hydrograph. *Water Resour. Res.* **1967**, *3*, 753–771. [[CrossRef](#)]
13. Olivera, F.; Maidment, D.R. Geographic information systems (GIS)-based spatially distributed model for runoff routing. *Water Resour. Res.* **1999**, *35*, 1155–1164. [[CrossRef](#)]
14. Hromadka, T.V., II; McCuen, R.H.; Yen, C.C. Comparison of overland flow hydrograph models. *ASCE J. Hydraul. Eng.* **1987**, *113*, 1422–1439. [[CrossRef](#)]
15. Su, D.; Fang, X. Estimating traveling time of flat terrain by 2-dimensional overland flow model. In Proceedings of the International Symposium on Shallow Flows, Delft University of Technology, Delft, The Netherlands, 16–18 June 2003.
16. Niri, M.Z.; Saghafian, B.; Golian, S.; Moramarco, T.; Shamsai, A. Derivation of travel time based on diffusive wave approximation for the time-area hydrograph simulation. *J. Hydrol. Eng.* **2012**, *17*, 85–91. [[CrossRef](#)]
17. Gourbesville, P.; Cunge, J.; Caignaert, G. *Advances in Hydroinformatics-Simhydro 2014*, 1st ed.; Springer: Singapore, 2014; p. 624.
18. Teng, J.; Jakeman, A.; Vaze, J.; Croke, B.F.; Dutta, D.; Kim, S. Flood inundation modelling: A review of methods, recent advances and uncertainty analysis. *Environ. Model. Softw.* **2017**, *90*, 201–216. [[CrossRef](#)]
19. Akan, A.O. Similarity solution of overland flow on pervious surface. *J. Hydraul. Eng.* **1985**, *111*, 1057–1067. [[CrossRef](#)]
20. Deng, Z.Q.; De Lima, J.L.M.P.; Singh, V.P. Transport rate-based model for overland flow and solute transport: Parameter estimation and process simulation. *J. Hydrol.* **2005**, *315*, 220–235. [[CrossRef](#)]
21. Hamouda, B.; Lahbassi, O. Integration of pervious area stream flow in urban hydrological model. *Energy Procedia* **2012**, *18*, 1573–1582. [[CrossRef](#)]
22. García Serrana, M.; Gulliver, J.S.; Nieber, J.L. Non-uniform overland flow-infiltration model for roadside swales. *J. Hydrol.* **2017**, *552*, 586–599. [[CrossRef](#)]
23. Hjelmfelt, A. Influence of infiltration on overland flow. *J. Hydrol.* **1978**, *36*, 179–185. [[CrossRef](#)]
24. Akan, A.O. Time of concentration formula for pervious catchments. *J. Irrig. Drain. Eng.* **1989**, *115*, 733–735. [[CrossRef](#)]
25. Suk, H.; Yeh, G.T. Development of particle tracking algorithms for various types of finite elements in multi-dimensions. *Comput. Geosci.* **2010**, *36*, 564–568. [[CrossRef](#)]
26. Schafer-Perini, A.L.; Wilson, J.L. Efficient and accurate front tracking for two-dimensional groundwater flow models. *Water Resour. Res.* **1991**, *27*, 1471–1485. [[CrossRef](#)]
27. Bensabat, J.; Zhou, Q.; Bear, J. An adaptive pathline-based particle tracking algorithm for the eulerian-lagrangian method. *Adv. Water Resour.* **2000**, *23*, 383–397. [[CrossRef](#)]
28. Cheng, H.P.; Cheng, J.R.; Yeh, G.T. A particle tracking technique for the lagrangian-eulerian finite element method in multi-dimensions. *Int. J. Numer. Methods Eng.* **1996**, *39*, 1115–1136. [[CrossRef](#)]
29. KC, M.; Fang, X. Estimating time parameters of overland flow on impervious surfaces by the particle tracking method. *Hydrol. Sci. J.* **2015**, *60*, 294–310. [[CrossRef](#)]
30. Delestre, O.; Darboux, F.; James, F.; Lucas, C.; Laguerre, C.; Cordier, S. FullSWOF: A free software package for the simulation of shallow water flows. *arXiv* **2014**. preprint arXiv:1401.4125.
31. Barré de Saint-Venant, A.J.C. Théorie du mouvement non permanent des eaux, avec application aux crues des rivières et à l'introduction des marées dans leurs lits. *Comptes Rendus des Séances de l'Académie des Sci.* **1871**, *73*, 237–240.
32. Zhang, W.; Cundy, T.W. Modeling of two-dimensional overland flow. *Water Resour. Res.* **1989**, *25*, 2019–2035. [[CrossRef](#)]
33. Audusse, E.; Bouchut, F.; Bristeau, M.-O.; Klein, R.; Perthame, B.T. A fast and stable well-balanced scheme with hydrostatic reconstruction for shallow water flows. *SIAM J. Sci. Comput.* **2004**, *25*, 2050–2065. [[CrossRef](#)]
34. Unterweger, K.; Wittmann, R.; Neumann, P.; Weinzierl, T.; Bungartz, H.-J. Integration of FullSWOF\_2D and PeanoClaw: Adaptivity and local time-stepping for complex overland flows. In *Recent Trends in Computational Engineering-CE2014*; Springer: Cham, Switzerland, 2015; pp. 181–195.

35. Cordier, S.; Coullon, H.; Delestre, O.; Laguerre, C.; Le, M.H.; Pierre, D.; Sadaka, G. FullSWOF paral: Comparison of two parallelization strategies (MPI and SkelGIS) on a software designed for hydrology applications. In *ESAIM: Proceedings*; EDP Sciences: Les Ulis, France, 2013; pp. 59–79.
36. Esteves, M.; Faucher, X.; Galle, S.; Vauclin, M. Overland flow and infiltration modelling for small plots during unsteady rain: Numerical results versus observed values. *J. Hydrol.* **2000**, *228*, 265–282. [[CrossRef](#)]
37. Bouchut, F. *Nonlinear Stability of Finite Volume Methods for Hyperbolic Conservation Laws and Well-Balanced Schemes for Sources*; Springer Science & Business Media: Berlin, Germany, 2004.
38. Delestre, O.; Lucas, C.; Ksinant, P.A.; Darboux, F.; Laguerre, C.; Vo, T.N.; James, F.; Cordier, S. Swashes: A compilation of shallow water analytic solutions for hydraulic and environmental studies. *Int. J. Numer. Methods Fluids* **2013**, *72*, 269–300. [[CrossRef](#)]
39. Abily, M.; Delestre, O.; Amossé, L.; Bertrand, N.; Laguerre, C.; Duluc, C.-M.; Gourbesville, P. Use of 3D classified topographic data with FullSWOF for high resolution simulation of a river flood event over a dense urban area. *arXiv* **2016**, arXiv:1603.07463.
40. Abily, M.; Bertrand, N.; Delestre, O.; Gourbesville, P.; Duluc, C.-M. Spatial global sensitivity analysis of high resolution classified topographic data use in 2D urban flood modelling. *Environ. Model. Softw.* **2016**, *77*, 183–195. [[CrossRef](#)]
41. Cordes, C.; Kinzelbach, W. Continuous groundwater velocity fields and path lines in linear, bilinear, and trilinear finite elements. *Water Resour. Res.* **1992**, *28*, 2903–2911. [[CrossRef](#)]
42. Pollock, D.W. *User's Guide for MODPATH/MODPATH-PLOT, Version 3: A Particle Tracking Post-Processing Package for MODFLOW, the U.S. Geological Survey Finite-Difference Ground-Water Flow Model*; U.S. Geological Survey: Reston, VA, USA, 1994; pp. 4–9.
43. Lu, N. A semianalytical method of path line computation for transient finite-difference groundwater flow models. *Water Resour. Res.* **1994**, *30*, 2449–2459. [[CrossRef](#)]
44. *Matlab and Statistics Toolbox Release 2017a*; The MathWorks Inc.: Natick, MA, USA, 2017.
45. Peugeot, C.; Esteves, M.; Galle, S.; Rajot, J.-L.; Vandervaere, J. Runoff generation processes: Results and analysis of field data collected at the east central supersite of the hapex-sahel experiment. *J. Hydrol.* **1997**, *188*, 179–202. [[CrossRef](#)]
46. Nash, J.E.; Sutcliffe, J.V. River flow forecasting through conceptual models part I—A discussion of principles. *J. Hydrol.* **1970**, *10*, 282–290. [[CrossRef](#)]
47. Rawls, W.J.; Brakensiek, D.L.; Miller, N. Green-Ampt infiltration parameters from soils data. *J. Hydraul. Eng.* **1983**, *109*, 62–70. [[CrossRef](#)]
48. KC, M.; Fang, X.; Yi, Y.-J.; Li, M.-H.; Thompson, D.B.; Cleveland, T.G. Improved time of concentration estimation on overland flow surfaces including low-sloped planes. *J. Hydrol. Eng.* **2014**, *19*, 495–508. [[CrossRef](#)]
49. Viessman, W.; Lewis, G.L. *Introduction to Hydrology*, 5th ed.; Pearson Education: Upper Saddle River, NJ, USA, 2003; p. 612.
50. Henderson, F.M.; Wooding, R.A. Overland flow and groundwater flow from a steady rainfall of finite duration. *J. Geophys. Res.* **1964**, *69*, 1531–1540. [[CrossRef](#)]
51. Morgali, J.R.; Linsley, R.K. Computer analysis of overland flow. *J. Hydraul. Div.* **1965**, *91*, 81–100.
52. Kirpich, Z.P. Time of concentration of small agricultural watersheds. *Civ. Eng.* **1940**, *10*, 362.
53. Johnstone, D.; Cross, W.P. *Elements of Applied Hydrology*; Ronald Press: New York, NY, USA, 1949.
54. Linsley, R.K.; Kohler, M.A.; Paulhus, J.L.H. *Hydrology for Engineers*; McGraw Hill Publications: New York, NY, USA, 1958.
55. Diskin, M.; Nazimov, N. Ponding time and infiltration capacity variation during steady rainfall. *J. Hydrol.* **1996**, *178*, 369–380. [[CrossRef](#)]
56. Chow, V.T.; Maidment, D.R.; Mays, L.W. *Applied Hydrology*, 2nd ed.; McGraw Hill: New York, NY, USA, 1988.

